Evaluation of Resonance Phenomena in Chaotic States through Typical Routes in Izhikevich Neuron Model

Sou Nobukawa[†], Haruhiko Nishimura[‡], Teruya Yamanishi[†] and Jian-Qin Liu[‡]

[†]Department of Management Information Science, Fukui University of Technology
3–6–1 Gakuen, Fukui, Fukui, 910–8505 Japan
Email: nobukawa@fukui-ut.ac.jp, yamanisi@fukui-ut.ac.jp
[‡]Graduate School of Applied Informatics, University of Hyogo
7–1–28, Minatojima-minamimachi, Chuo-ku, Kobe, Hyogo, 650–8588 Japan
Email: haru@ai.u-hyogo.ac.jp, jian-qin.liu@hotmail.com

Abstract—Over the past few decades, a considerable number of studies have been conducted on bifurcation and chaos in spiking neuron models. Among them, Izhikevich neuron model as a hybrid neuron model can induce many kinds of bifurcation behaviors and reproduce almost spiking activities observed in the actual neural systems. Chaotic resonance (CR) in which a system responds to a weak signal by the effect of chaotic activities is known as one of the functionality of chaos in neural systems. At this stage, there have been few studies that examine the efficiencies of signal response in CR in spiking neural systems with discontinuous after-spike resetting process. Thus, in this paper, focusing on Izhikevcih neuron model, we compare the characteristics of CR in the chaotic states arising through period-doubling bifurcation route and intermittency route to chaos.

1. Introduction

Chaotic resonance (CR) in which a system responds to a weak signal by the effect of chaotic activities is known as one of the functionality of chaos in neural systems [1, 2]. In the CR phenomenon in spiking neural systems, chaotic behavior leads to the generation of spikes not at specific times, but at varying scatter times for each trial by input signals. Thus, the frequency distribution of these spike timings against the input signal becomes congruent with the shape of the input signal [2].

Over the past few decades, a considerable number of studies have been conducted on chaos and bifurcation in spiking neural systems, such as Hodgkin-Huxley type model, FitzHugh-Nagumo model and Hindmarsh-Rose model [3]. Most notably, Izhikevich neuron model as a hybrid neuron model, combining continuous spike generation mechanism and discontinuous after-spike resetting process, can induce many kinds of bifurcation and reproduce almost all spiking activities observed in the actual neural systems by tuning a few parameters [4]. The variety of reproduced spiking patterns is high in comparison with other spiking neuron models [5].

Furthermore, some methods to evaluate chaotic behaviors in the hybrid neuron system including state dependent jump in its resetting process were developed recently, such as bifurcation analysis on the Poincaré section and Lyapunov exponent with a saltation matrix on the system trajectory [6, 7]. With the aid of them, we have revealed that there exist the period-doubling bifurcation and the intermittency route to chaos in different regions of parameters in Izhikevich neuron model [8]. First one is the region around the parameter sets for typical spiking patterns observed in cerebral cortex [4]. Second one is the region including the parameter set for chaotic spiking previously presented by Izhikevich [5]. At this stage, the signal response of CR has not been evaluated yet in the chaotic states produced through these different routes. Thus, in this paper, we focus on these typical routes to chaos in the Izhikevich neuron model and evaluate their signal responses in CR.

2. Model and Method

2.1. Izhikevich neuron model

Izhikevich neuron model [4, 5] consists of two-dimensional ordinary differential equations of the form

$$\dot{v} = 0.04v^2 + 5v + 140 - u + I, \qquad (1)$$
$$\dot{u} = a(bv - u), \qquad (2)$$

with the auxiliary after-spike resetting

$$\text{if } v \geq 30[\text{mV}], \text{ then } \begin{cases} v \leftarrow c \\ u \leftarrow u + d. \end{cases} \qquad (3)$$

Here, v and u represent the membrane potential of a neuron and the membrane recovery variable, respectively. The parameters a and b describe the time scale and the sensitivity of u, respectively. I is the input dc-current. To examine its response against a weak

periodic signal $S(t) = A\sin(2\pi f_0 t)$, we extend Eq. (1) as follows:

$$\dot{v} = 0.04v^2 + 5v + 140 - u + I + S(t). \tag{4}$$

Note that the sinusoidal signal is utilized merely as a typical example of a signal in a neural system.

2.2. Evaluation indexes

2.2.1. Indexes for evaluation of chaos and bifurcation

To quantify the chaotic activity in Izhikevich neuron model, the Lyapunov exponent with a saltation matrix is utilized. On a system with a continuous trajectory between the i-th and the $(i+1)$-th spiking times ($t_i \leq t \leq t_{i+1}$), the variational equations of Eqs. (1) and (2) are defined as follows:

$$\dot{\Phi}_{i+1}(t, t_i) = J(v, u, t)\Phi_{i+1}(t, t_i), \tag{5}$$
$$\Phi_{i+1}(t_i, t_i) = E, \tag{6}$$

where, Φ, J, and E indicate the state transition matrix, the Jacobian matrix, and a unit matrix, respectively. At $t = t_i$, the saltation matrix is given by

$$S_i = \begin{bmatrix} \frac{\dot{v}^+}{\dot{v}^-} & 0 \\ \frac{\dot{u}^+ - \dot{u}^-}{\dot{v}^-} & 1 \end{bmatrix}, \tag{7}$$

In the above, (v^-, u^-) and (v^+, u^+) represent the values of (v, u) before and after spiking, respectively. In case spikes arise in the range $[T^k : T^{k+1}]$ [ms], $\Phi^k(T^{k+1}, T^k)$ ($k = 0, 1, \cdots, N-1$) [7] can be expressed as

$$\Phi^k(T^{k+1}, T^k) = \Phi_{i+1}(T^{k+1}, t_i)S_i\Phi_i(t_i, t_{i-1})$$
$$\cdots S_2\Phi_2(t_2, t_1)S_1\Phi_1(t_1, T^k). \tag{8}$$

Based on the eigenvalues l_j^k ($j = 1, 2$) of $\Phi^k(T^{k+1}, T^k)$, the Lyapunov spectrum λ_j is calculated by

$$\lambda_j = \frac{1}{T^N - T^0} \sum_{k=0}^{N-1} \log(|l_j^k|). \tag{9}$$

In our simulation, we set $T^{k+1} - T^k$ as the time required for 20 spikes ($i = 20$). We set 1000 [ms] as the maximum value in case $T^{k+1} - T^k$ takes 1000 [ms] before 20 spikes occur.

In order to conduct bifurcation analysis in the system with a state-dependent jump, we set a Poincaré section $\Phi(v = 30)$. The dynamics of system behavior on Φ are given by Poincaré map ϕ. In the literature [6], the stability of a fixed point $u_0 = \phi^l(u_0)$ ($l = 1, 2, \cdots$) are evaluated by

$$\mu = \frac{\partial \phi^l}{\partial \mathbf{u}_0} = \begin{pmatrix} 0 & 1 \end{pmatrix} \begin{pmatrix} 0 & 0 \\ -\dot{v}/\dot{u} & 1 \end{pmatrix} \Phi(t_l, t_0) \begin{pmatrix} 0 \\ 1 \end{pmatrix}. \tag{10}$$

Here, $\mathbf{u}_0 = (v_0, u_0)$ indicates the initial value of orbit $\mathbf{u} = (v, u)$ at $t = t_0$. $|\mu < 1|$, $\mu = -1$, and $\mu = 1$ represent the stable condition, period doubling bifurcation, and tangent bifurcation, respectively.

2.2.2. Indexes for evaluation of signal response

To examine the signal response, we calculate the timing of the spikes against signal $S(t)$ by using a cycle histogram $F(\tilde{t})$ [10]. $F(\tilde{t})$ is a histogram of firing counts at $t_k \mod (T_0)$ ($k = 1, 2, \cdots$) against signal $S(\tilde{t})$ with period $T_0(= 1/f_0)$, $0 \leq \tilde{t} \leq T_0$. For example, for $T_0 = 10$, in case the spike times are $t_k = 2, 6, 12, 16, 26$, the values of $t_k \mod (T_0)$ are $2, 6, 2, 6, 6$. The cycle histogram then becomes $F(2) = 2$ and $F(6) = 3$. Furthermore, we use the mutual correlation $C(\tau)$ between the cycle histogram $F(\tilde{t})$ of the neuron spikes and the signal $S(\tilde{t})$ as follows:

$$C(\tau) = \frac{C_{SF}(\tau)}{\sqrt{C_{SS}C_{FF}}}, \tag{11}$$

$$C_{SF}(\tau)$$
$$= <(S(\tilde{t} + \tau) - <S(\tilde{t})>)(F(\tilde{t}) - <F(\tilde{t})>)>, \tag{12}$$

$$C_{SS} = <(S(\tilde{t}) - <S(\tilde{t})>)^2>, \tag{13}$$
$$C_{FF} = <(F(\tilde{t}) - <F(\tilde{t})>)^2>. \tag{14}$$

For the time delay factor τ caused by the spike latency against $S(t)$, we check $\max_\tau C(\tau)$, i.e., the largest $C(\tau)$ between $0 \leq \tau \leq T_0$.

3. Results and Evaluations

3.1. Parameter regions to evaluate signal response

At first, we introduce the parameter regions where a chaotic state arises. Left-sided figures in Figs. 1 (a) and (b) show the dependencies of maximum Lyapunov exponent λ_1 on parameters of c and d in the region around parameter sets for the spiking patterns of regular spiking (RS), intrinsically bursting (IB) and chattering (CH) (see right-sided figure in Fig. 1 (a)) and the region including the parameter set previously shown by Izhikevich for chaotic spiking (see right-sided figure in Fig. 1 (b)), respectively. The chaotic states ($\lambda_1 > 0$) exist in $-59 \lesssim c \lesssim -40$, $d \approx 1.0$ in the former case and $d \lesssim -13$ in the latter case. As the parameter regions for evaluating CR, we chose $0.82 \leq d \leq 0.92$ in the former region, and $-15.5 \leq d \leq -11$ in the latter region, hereinafter called region #1 and #2, respectively. Figure 2 indicates the bifurcation diagram (black dots) and Lyapunov exponents (red dotted ($j = 1$) and green dashed
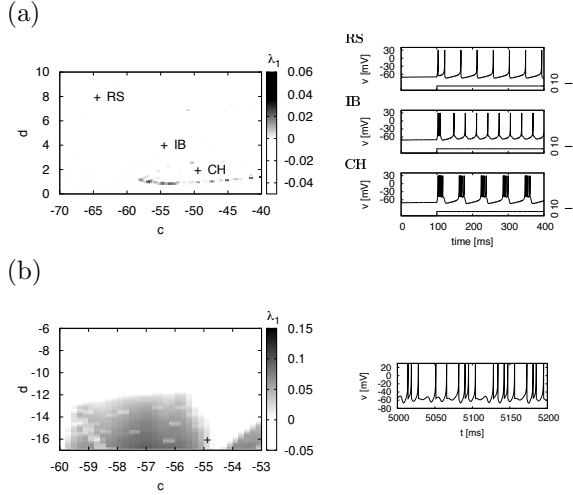
Figure 1: Dependence of maximum Lyapunov exponent λ_1 on parameters c and d. (a) Region around parameter sets for RS, IB and CH. The symbols of ($+$) indicate the parameter sets for RS and IB, CH ($a = 0.02, b = 0.2, I = 10$). (b) Region around parameter set proposed by Izhikevich for chaotic spiking. The symbol of ($+$) indicates the parameter set for chaotic spiking ($a = 0.2, b = 2, I = -99$). These figures are quoted from Ref. [8].

Figure 2: Bifurcation diagram of u_i and Lyapunov exponents λ_j ($j = 1, 2$). (a) Period-doubling bifurcation case (called region #1) ($a = 0.02, b = 0.2, c = -55, I = 10$). (b) Tangent bifurcation case (called region #2) ($a = 0.2, b = 2, c = -56, I = -99$).

($j = 2$) lines) as functions of parameter d in region #1 case ((a)) and region #2 case ((b)). In Fig. 2 (a), the period-doubling bifurcation ($\mu = -1$) arises at $d = 0.8348, 0.8828, 0.8916, 0.894$ and the chaotic state ($\lambda_1 > 0, \lambda_2 = 0$) appears $d \gtrsim 0.894$. Hence, the period-doubling bifurcation route to chaos exists in this region. While, in Fig. 2 (b), the tangent bifurcation ($\mu = 1$) arises at $d \approx -11.9$ and the chaotic state ($\lambda_1 > 0, \lambda_2 = 0$) appears. This chaotic state produced by tangent bifurcation indicates the intermittency chaos alternating laminar and turbulent modes in a general way [11]. That is, the intermittency route to chaos exists in this region.

3.2. Signal response in chaotic resonance

In the above mentioned chaotic parameter regions #1 and #2, we evaluate the response against a weak signal ($A = 10^{-2}, f_0 = 0.1$). Figures 3 (a) and (b) show the dependence of $\max_\tau C(\tau)$ (upper) and λ_j ($j = 1, 2$) (lower) on parameter d in the region #1 and #2, respectively. In the region #1 (Fig. 3 (a)), the neuron exhibits the periodic spiking ($\lambda_1 \approx 0, \lambda_2 < 0$) in $0.82 \lesssim d \lesssim 0.88$ and the chaotic spiking ($\lambda_1 > 0, \lambda_2 \approx 0$) in $0.88 \lesssim d \lesssim 0.92$. In the periodic spiking state, the value of $\max_\tau C(\tau)$ is less than 0.1. While in the chaotic spiking state, the value of $\max_\tau C(\tau)$ is higher in comparison with the periodic spiking state.
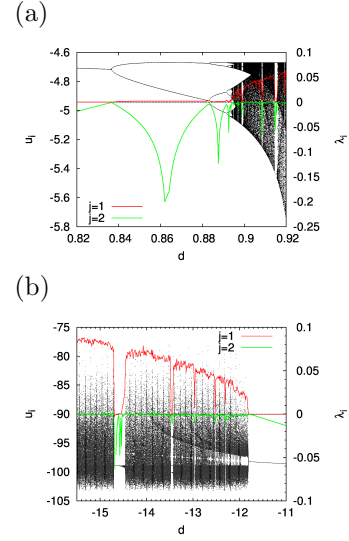
Especially, at $d \approx 0.89$ locating around the bifurcation to chaos called edge of chaos [12], $\max_\tau C(\tau)$ has a peak value (≈ 0.8). Thus, it can be interpreted that CR arises in chaotic region and this efficiency is maximized at edge of chaos. In the region #2 (Fig. 3 (b)), the chaotic spiking state ($\lambda_1 > 0, \lambda_2 \approx 0$) arises in $-15.5 \lesssim d \lesssim -12$ and $\max_\tau C(\tau)$ is high value by the effect of this chaotic spiking state. Also, the value of $\max_\tau C(\tau)$ indicates the similar tendency of region #1 (Fig. 3 (a)), i.e., at $d \approx -12.3$ locating the edge of chaos, $\max_\tau C(\tau)$ has a peak value (≈ 0.9).

Furthermore, Figs. 4 (a) and (b) show the scatter plots between $\max_\tau C(\tau)$ and λ_1 obtained in Figs.3 (a) (region #1 case) and (b) (region #2 case), respectively. The red dotted line indicates the mean value of $\max_\tau C(\tau)$ in the bin λ_1 with window $\Delta\lambda_1 = 0.005$. From these results, in both regions $\max_\tau C(\tau)$ has the peak at appropriate value of λ_1 ($\max_\tau C(\tau) \approx 0.7$ at $\lambda_1 \approx 0.03$ in the region #1 case and $\max_\tau C(\tau) \approx 0.9$ at $\lambda_1 \approx 0.04$ in the region #2 case). These peaks correspond to the points for the edge of chaos ($d \approx 0.89$ in region #1 and $d \approx -12.3$ in region #2) obtained Fig.3. Hence, the efficiency of signal response in CR has an unimodal maximum with respect to the stability for chaotic orbits represented by λ_1 and this peak locates in the edge of chaos.

4. Conclusions

In this paper, we showed two kinds of routes to chaos by using the Lyapunov exponent with saltation matrix
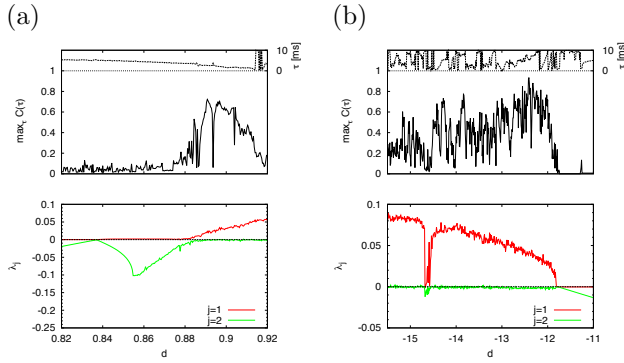
(a)　　　　　　　　(b)

Figure 3: Dependence of mutual correlation $\max_\tau C(\tau)$ (upper) and Lyapunov exponent λ_j ($j = 1, 2$) (lower) on parameter d. (a) Region #1 case. ($a = 0.02, b = 0.2, c = -55, I = 10$) (b) Region #2 case. ($a = 0.2, b = 2, c = -56, I = -99$)
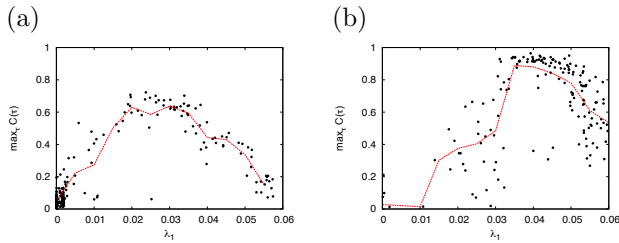

(a)　　　　　　　　(b)

Figure 4: Scatter plot between $\max_\tau C(\tau)$ and λ_1 obtained in Fig. 3 (red dotted line: mean value of $\max_\tau C(\tau)$ in the bin λ_1 with window $\Delta\lambda_1 = 0.005$). (a) Region #1 case. (b) Region #2 case.

and the index for stability of a fixed point on Poincaré section. One is the period-doubling bifurcation route to chaos and the other is the intermittency route to chaos. Under the condition of inputing a weak periodic signal, the enhancement of signal response by the effect of chaotic spikes, i.e., CR has been confirmed in the chaotic states induced by these routes to chaos. Furthermore, we revealed that the efficiency of signal response in CR has an unimodal maximum with respect to the stability for chaotic orbits and this peak locates in the edge of chaos.

In our future works, we will further examine the mechanism to achieve a high efficiency of signal response in the edge of chaos demonstrated in this study, comparing between the systems with/without discontinuous after-spike resetting process.

Acknowledgments

References

[1] H. Nishimura, N. Katada and K. Aihara, "Coherent Response in a Chaotic Neural Network", Neural Processing Letters, vol.12, no.1, pp.49–58, 2000.

[2] N. Schweighofer, K. Doya, H. Fukai, J. V. Chiron, T. Furukawa, M. Kawato, "Chaos may enhance information transmission in the inferior olive", Proceedings of the National Academy of Sciences, vol.101, no.13, pp.4655–4660, 2004

[3] M.I. Rabinovich, P. Varona, A.I. Selverston, H.D.I. Abarbanel, "Dynamical principles in neuroscience", Reviews of Modern Physics, vol.78, no.4, pp.1213–1265, 2006.

[4] E.M. Izhikevich, "Simple Model of Spiking Neurons", IEEE Transactions on Neural Networks, vol.14, no.6, pp.1569–1572, 2003.

[5] E.M. Izhikevich, "Which Model to Use for Cortical Spiking Neurons?", IEEE Transactions on Neural Networks, vol.15, no.5, pp.1063–1070, 2004.

[6] A. Tamura, T. Ueta, S. Tsuji, "Bifurcation analysis of Izhikevich neuron model", Dynamics of continuous, discrete and impulsive systems, Series A: mathematical analysis, vol.16, no.6, pp.849–862, 2009.

[7] F. Bizzarri, A. Brambilla, G.S. Gajani, "Lyapunov exponents computation for hybrid neurons", J. Comput. Neurosci., vol.35, no.2, pp.201–212, 2013.

[8] S. Nobukawa, H. Nishimura, T. Yamanishi, J.-Q. Liu, "Chaotic States Induced by Resetting Process in Izhikevich Neuron Model", Journal of Artificial Intelligence and Soft Computing Research, vol.5, no.2, pp.109–119, 2015.

[9] P. Berge, Y. Pomeau, C. Vidal, Order in chaos, The Deterministic Approach to Turbulence, 1984.

[10] S. Nobukawa, H. Nishimura, "Signal Response in Velarde-Llinás Model of Inferior Olive Neuron", IEICE, vol.J96.A, no.1, pp.1–11 (in Japanese), 2013.

[11] H. Nagashima, Y. Baba, Introduction to chaos: physics and mathematics of chaotic phenomena, CRC Press, 1998.

[12] C.G. Langton, "Computation at the edge of chaos: phase transitions and emergent computation", Physica D: Nonlinear Phenomena, vol.42, no.1, pp.12–37, 1990.